

# Resonant forcing of multi-dimensional chaotic map dynamics

Glenn Foster, Alfred W. Hübler, and Karin Dahmen

*Department of Physics, University of Illinois at Urbana-Champaign, Urbana, Illinois 61801\**

(Dated: February 4, 2007)

## Abstract

We study resonances of chaotic map dynamics. We use the calculus of variations to determine the additive forcing function that induces the largest response. We find that resonant forcing functions complement the separation of nearby trajectories, in that the product of the displacement of nearby trajectories and the resonant forcing is a conserved quantity. As a consequence, the resonant function will have the same periodicity as the displacement dynamics and if the displacement dynamics are irregular, then the resonant forcing function will be irregular as well. Furthermore we show that resonant forcing functions of chaotic systems decrease exponentially, where the rate equals the negative of the largest Lyapunov exponent of the unperturbed system. We compare the response to optimal forcing with random forcing, and find that the optimal forcing is particularly effective if the largest Lyapunov exponent is significantly larger than the other Lyapunov exponents. However, if the largest Lyapunov exponent is much larger than unity, then the optimal forcing decreases rapidly and is only as effective as a single push forcing.

PACS numbers: 05.45.-a, 02.30.Xx, 45.10.Hj

---

\*Electronic address: a-hubler@uiuc.edu

## I. INTRODUCTION

Resonance phenomena of sinusoidally driven damped nonlinear oscillators have been widely studied [1–3] and have numerous applications including nonlinear response phenomena [4, 5], stochastic resonance [6], and nonlinear transport phenomena [7]. Less studied are periodically driven chaotic systems [8]. An area that has received much less attention are resonance phenomena of nonlinear systems due to aperiodic and chaotic forcing functions. Ott, Grebogy, and York showed in 1990 [9] that a chaotic system can be steered toward periodic orbits with small controls and Baba et al. [10] showed in 2002 that chaos can be effectively controlled with delayed feedback. More recently Soskin et al. [11, 12] found that small changes in the Hamiltonian of a dynamical system can create a large response. Plapp [13] and others [14, 15] used the calculus of variations to show that a special class of aperiodic driving forces can achieve a large energy transfer to a nonlinear oscillator. Such non-sinusoidal resonant forcing functions yield a high signal-to-noise ratio, which can be used for system identification with general resonance spectroscopy [16]. The non-sinusoidal resonant forcing functions have the same dynamics as the time reflected transient dynamics of the unperturbed system [15].

In this paper, we present a methodology to determine resonant forcing functions for chaotic systems. We show analytically that resonant driving forces for chaotic map dynamics are closely related to the unperturbed dynamics of the system. Further, we show that resonant forcing functions decrease exponentially, where the rate is equal to the largest Lyapunov exponent of the unperturbed system. We illustrate that resonant forcing functions yield a large response, even if the initial condition of the system is not exactly known.

## II. RESONANT FORCING FUNCTION

We consider the iterated map dynamics

$$\mathbf{x}^{(n+1)} = \mathbf{f}(\mathbf{x}^{(n)}) + \mathbf{F}^{(n)} \quad (2.1)$$

where  $\mathbf{x}^{(n)} \in \mathbb{R}^d$  denotes the state of the  $d$ -dimensional system at time step  $n = 0, 1, \dots, N - 1$  and  $\mathbf{F}^{(n)} \in \mathbb{R}^d$  the forcing function at time step  $n$ . The magnitude of the forcing function

is defined as

$$F^2 = \sum_{n=0}^{N-1} (\mathbf{F}^{(n)})^2 \quad (2.2)$$

The final response to the forcing is defined as

$$R^2 = (\mathbf{x}^{(N)} - \mathbf{y}^{(N)})^2 \quad (2.3)$$

where  $\mathbf{y}^{(n+1)} = \mathbf{f}(\mathbf{y}^{(n)})$  is the unperturbed dynamics with  $\mathbf{y}^{(0)} = \mathbf{x}^{(0)}$ . We use the calculus of variations with Lagrange function  $L$  [17] to determine the forcing function which yields the largest response  $R$ , where  $L$  is

$$L = \frac{R^2}{2} + \sum_{n=0}^{N-1} \mathbf{k}^{(n)} (\mathbf{x}^{(n+1)} - \mathbf{f}(\mathbf{x}^{(n)}) - \mathbf{F}^{(n)}) + \frac{\mu}{2} (\mathbf{F}^{(n)})^2 \quad (2.4)$$

and where  $\mathbf{k}^{(n)}$  and  $\mu$  are Lagrange multipliers. The stationary points of the Lagrange function provide a necessary condition for the maximum response. At stationary points the partial derivatives with respect to the components of the independent variables  $\mathbf{x}^{(n)} = (x_1^{(n)}, x_2^{(n)}, \dots, x_d^{(n)})$  and  $\mathbf{F}^{(n)} = (F_1^{(n)}, F_2^{(n)}, \dots, F_d^{(n)})$  are equal to zero.  $\partial L / \partial x_i^{(n)} = 0$ , and  $\partial L / \partial F_i^{(n)} = 0$  for  $n = 0, 1, \dots, N - 1$  yield:

$$\begin{aligned} (J^{(n+1)})^T \mathbf{k}^{(n+1)} - \mathbf{k}^{(n)} &= 0 \\ \mu \mathbf{F}^{(n)} - \mathbf{k}^{(n)} &= 0 \end{aligned} \quad (2.5)$$

for  $n = 0, 1, \dots, N - 1$ , where  $J^{(n)} = (\partial f_i / \partial x_j)|_{\mathbf{x}^{(n)}}$  is the Jacobi matrix evaluated at  $\mathbf{x}^{(n)}$ . The superscript  $T$  indicates the transpose operator.  $\partial L / \partial x_i^{(N)} = 0$  and  $\partial L / \partial x_i^{(N)} = 0$  yields:

$$\mathbf{x}^{(N)} - \mathbf{y}^{(N)} + \mathbf{k}^{(N-1)} = 0 \quad (2.6)$$

Elimination of the Lagrange multipliers  $\mathbf{k}^{(n)}$  from Eq. (2.5) defines the dynamics of the resonant forcing function

$$(J^{(n+1)})^T \mathbf{F}^{(n+1)} = \mathbf{F}^{(n)} \quad (2.7)$$

where  $n=0,1,\dots,N-1$ , and the Eq. (2.6) reads

$$\mathbf{x}^{(N)} - \mathbf{y}^{(N)} = -\mu \mathbf{F}^{(N-1)} \quad (2.8)$$

Eq. (2.8) can be used to determine a boundary condition for the mapping function given by Eq. (2.7). The control is stable if the displacement between nearby trajectories decreases on

average. The dynamics of a small displacement  $\mathbf{d}^{(n)} = \mathbf{x}^{(n)} - \tilde{\mathbf{x}}^{(n)}$  between two neighboring trajectories at  $\mathbf{x}^{(n)}$  and  $\tilde{\mathbf{x}}^{(n)}$  (from Taylor expanding Eq. (2.1)) is given by

$$\mathbf{d}^{(n+1)} = J^{(n)} \mathbf{d}^{(n)} \quad (2.9)$$

Next we transpose Eq. (2.7) and multiply with  $\mathbf{d}^{(n+1)}$

$$(\mathbf{F}^{(n+1)})^T J^{(n+1)} \mathbf{d}^{(n+1)} = \mathbf{F}^{(n)} \cdot \mathbf{d}^{(n+1)} \quad (2.10)$$

and with Eq. (2.9) we obtain

$$\mathbf{F}^{(n+1)} \cdot \mathbf{d}^{(n+2)} = \mathbf{F}^{(n)} \cdot \mathbf{d}^{(n+1)} \quad (2.11)$$

Hence the scalar product of the resonant forcing and the displacement is a conserved quantity

$$P = \mathbf{F}^{(n)} \cdot \mathbf{d}^{(n+1)} \quad (2.12)$$

for  $n = 0, 1, \dots, N - 1$ .  $P$  is conserved no matter if the unperturbed dynamics is periodic or chaotic. The constant  $P$  depends on the magnitude of the forcing function  $F$ . If the system is one-dimensional, then the resonant forcing is proportional to the inverse of the displacement at each time step, i.e.  $F^{(n)} = P/d^{(n+1)}$ . If an initial displacement  $\mathbf{d}^{(1)}$  is perpendicular to the initial resonant forcing  $\mathbf{F}^{(0)}$ , i.e.  $P = 0$ , then the resonant forcing function stays perpendicular to the images of this initial displacement, i.e.

$$\mathbf{F}^{(n)} \cdot \mathbf{d}^{(n+1)} = 0 \text{ if } \mathbf{F}^{(0)} \cdot \mathbf{d}^{(1)} = 0 \quad (2.13)$$

for  $N = 1, 2, \dots, N - 1$ . Figure 1 shows the relative magnitude  $F^{(n)}/F$  and direction  $\phi^{(n)} = \arctan(F_2^{(n)}/F_1^{(n)})$  of the resonant forcing function for a chaotic Henon map dynamics  $x_1^{(n+1)} = 1 - 1.1(x_1^{(n)})^2 + x_2^{(n)} + F_1^{(n)}$ ,  $x_2^{(n+1)} = 0.3x_1^{(n)} + F_2^{(n)}$  for  $n = 0, 1, 2$ ,  $F = 0.1$ ,  $x_1^{(0)} = -0.3$ , and  $x_2^{(0)} = 0.3$ . The Henon map is a time discrete version of the Lorenz attractor. In 1963, Edward Lorenz derived this dynamical system from the simplified equations of convection rolls arising in the equations of the atmosphere. We solve Eq. (2.1), Eq. (2.2), Eq. (2.7), and Eq. (2.8) numerically with one percent accuracy. These equations have two or more solutions. At some solutions the response reaches a maximum, at others it reaches a minimum. We determine the response for each solution numerically and choose the solution with the largest response. We find that the quantity  $P$  (see Eq. (2.12)) is equal to zero for  $n = 0, 1, 2$  and that all displacements  $\mathbf{d}^{(n+1)}$  are perpendicular to the forces  $\mathbf{F}^{(n)}$ , if the

direction of the initial displacement  $\mathbf{d}^{(1)}$  is perpendicular to  $\mathbf{F}^{(0)}$ , i.e.  $d_1^{(1)} = \cos(\phi^{(0)} + \pi/2)$  and  $d_2^{(1)} = \sin(\phi^{(0)} + \pi/2)$ . If the initial displacement has a different direction,  $P$  is typically not zero but it stays constant within the numerical accuracy of the computation.

### III. RESONANT FORCING FUNCTIONS WITH SMALL MAGNITUDE

Next we assume that the forcing function is small and expand the Jacobi matrix about the unperturbed dynamics to lowest order, i.e.  $J^{(n)} \approx (\partial f_i / \partial x_j)|_{\mathbf{y}^{(n)}}$ . We iterate and expand Eq. (2.1). To lowest order the difference between the trajectory of the driven system and the unperturbed system reads:

$$\mathbf{x}^{(N)} - \mathbf{y}^{(N)} = \mathbf{F}^{(N-1)} + J^{(N-1)}\mathbf{F}^{(N-2)} + J^{(N-1)}J^{(N-2)}\mathbf{F}^{(N-3)} + \dots + J^{(N-1)}\dots J^{(1)}\mathbf{F}^{(0)} \quad (3.1)$$

With Eq. (2.7) we obtain (see Eq. (D.1) in the Appendix)

$$\mathbf{x}^{(N)} - \mathbf{y}^{(N)} = M\mathbf{F}^{(N-1)} \quad (3.2)$$

where  $M^{(n)} = J^{(N-1)}\dots J^{(N-n)}(J^{(N-n)})^T\dots(J^{(N-1)})^T$  and  $M = I + \sum_{n=1}^{N-1} M^{(n)}$ .  $I$  is the identity matrix. With Eq. (2.8) this becomes

$$M\mathbf{F}^{(N-1)} = -\mu\mathbf{F}^{(N-1)} \quad (3.3)$$

where  $M$  is a symmetric matrix with up to  $d$  orthogonal eigenvectors  $\mathbf{e}_i$ , where  $M\mathbf{e}_i = \mu_i\mathbf{e}_i$ ,  $i = 1, 2, \dots, d$  and  $\mathbf{e}_i^2 = 1$ . The corresponding eigenvalues  $\mu_i$  are positive. The eigenvectors of matrix  $M$  are the solutions of Eq. (3.3)  $\mathbf{F}^{(N-1)} = \pm F^{(N-1)}\mathbf{e}_i$ , where  $F^{(N-1)} = |\mathbf{F}^{(N-1)}|$  and  $\mu = -\mu_i$ . In the next few steps we determine which solutions maximize the response. Eq. (2.3), Eq. (2.8), and Eq. (3.3) yield

$$R^2 = (\mathbf{x}^{(N)} - \mathbf{y}^{(N)})^2 = \mu_i^2 (F^{(N-1)})^2 \quad (3.4)$$

Since we know that the final value of the forcing function is  $\mathbf{F}^{(N-1)} = \pm F^{(N-1)}\mathbf{e}_i$ , the other values of the resonant forcing function are

$$\begin{aligned} \mathbf{F}^{(n)} &= (J^{(n+1)})^T \mathbf{F}^{(n+1)} \\ &= (J^{(n+1)})^T (J^{(n+2)})^T \mathbf{F}^{(n+2)} \\ &= (J^{(n+1)})^T (J^{(n+2)})^T \dots (J^{(N-1)})^T \mathbf{F}^{(N-1)} \\ &= \pm |\mathbf{F}^{(N-1)}| (J^{(n+1)})^T (J^{(n+2)})^T \dots (J^{(N-1)})^T \mathbf{e}_i \end{aligned} \quad (3.5)$$

With this equation and the constraint (see Eq. (2.2)) we determine  $|\mathbf{F}^{(N-1)}|$  as a function of  $F^2$  (see Eq. (D.2) in the Appendix):

$$F^2 = \mu_i (F^{(N-1)})^2 \quad (3.6)$$

Hence  $F^{(N-1)} = F/\sqrt{\mu_i}$ . With Eq. (3.4) we find  $R^2 = \mu_i F^2$ . Hence the final forcing which parallels the eigenvector with the largest eigenvalue of  $M$ ,  $\hat{\mu} = \max\{\mu_i\}$  produces the largest response, and the largest response is

$$R^2 = \hat{\mu} F^2 \quad (3.7)$$

and with Eq. (3.5) we obtain

$$\hat{\mathbf{F}}^{N-1} = \pm \frac{F}{\sqrt{\hat{\mu}}} \hat{\mathbf{e}} \quad (3.8)$$

where  $\hat{\mathbf{e}}$  is the eigenvector that corresponds to the largest eigenvalue of  $M$ , and for  $n = 0, 1, \dots, N-2$ :

$$\mathbf{F}^{(n)} = \pm \frac{F}{\sqrt{\hat{\mu}}} (J^{(n+1)})^T \dots (J^{(N-2)})^T (J^{(N-1)})^T \hat{\mathbf{e}} \quad (3.9)$$

The response depends on the initial state  $\mathbf{x}^{(0)}$ . The expectation value of the response is

$$R^2 = F^2 \int \hat{\mu} \rho(\mathbf{x}) d\mathbf{x} \quad (3.10)$$

where  $\rho(\mathbf{x})$  is the equilibrium distribution of the attractor. Figure 2 shows the expectation value of the response of a chaotic Henon map dynamics (see Appendix A) as a function of the map parameter  $a$ , where  $b = 0.3$ . The numerical value is in good agreement with the theoretical value (Eq. (A.10)). In the chaotic regime ( $a > 1.06$ ) the function has many discontinuities, since the shape of the attractor changes suddenly and thus expectation value  $\langle (x_1^{(1)})^2 \rangle$  has many discontinuities as a function of  $a$ . The matrix  $M^{(n)}$  describes how the magnitude of a displacement grows

$$|\mathbf{d}^{(N)}|^2 = (J^{(N-1)} J^{(N-2)} \dots J^{(0)} \mathbf{d}^{(0)})^T (J^{(N-1)} J^{(N-1)} \dots J^{(0)} \mathbf{d}^{(0)}) = (\mathbf{d}^{(0)})^T M^{(N)} \mathbf{d}^{(0)}. \quad (3.11)$$

If  $\mu_i^{(n)}$  are the eigenvalues of  $M^{(n)}$  then the Lyapunov exponents are the limits  $\lambda_i = \lim_{n \rightarrow \infty} \frac{1}{2n} \ln \mu_i^{(n)}$ . The set of Lyapunov exponents will be the same for almost all starting points on an ergodic attractor. For some chaotic systems the matrices  $M^{(n)}$  have the same eigenvectors or approximately the same eigenvectors. For instance if the Jacobian is constant, i.e.  $J^{(n)} = J^{(0)}$  for  $n = 1, 2, \dots, N-1$ , then  $M^{(n)} = (J^{(0)})^n ((J^{(0)})^T)^n =$

$(J^{(0)}(J^{(0)})^T)^n = (M^{(1)})^n$  since  $J^{(0)}(J^{(0)})^T = (J^{(0)})^T J^{(0)}$ . This is the case for the shift map (Appendix B). If the matrices  $M^{(n)}$  have the same eigenvectors or approximately the same eigenvectors the eigenvalues obey the following relation

$$\mu_i^{(n)} \approx (\mu_i^{(1)})^n \approx e^{2n\lambda_i} \quad (3.12)$$

If an initial displacement is parallel to the eigenvector of  $M$  that corresponds to the largest Lyapunov exponent  $\hat{\lambda} = \max\{\lambda_i, i = 1, 2, \dots, d\}$ , then it has the largest growth rate, i.e.  $d^{(n)} = e^{n\hat{\lambda}}d^{(0)}$ . The final value of the optimal forcing function  $\mathbf{F}^{(N-1)}$  is parallel to the eigenvector of  $M$  that corresponds to the largest Lyapunov exponent and earlier values obey the dynamics (using Eq. (3.5)):

$$\begin{aligned} |\mathbf{F}^{(n)}|^2 &= \left( (J^{(n+1)})^T \dots (J^{(N-1)})^T \mathbf{F}^{(N-1)} \right)^T \left( (J^{(n+1)})^T \dots (J^{(N-1)})^T \mathbf{F}^{(N-1)} \right) \quad (3.13) \\ &= (\mathbf{F}^{(N-1)})^T M^{(N-n-1)} \mathbf{F}^{(N-1)} = \mu_i^{(N-n-1)} (F^{(N-1)})^2 = \frac{1}{\mu_i^n} (F^{(0)})^2 \end{aligned}$$

Hence the growth rate of the magnitude of the the optimal forcing function is equal to the opposite of the largest Lyapunov exponent:

$$F^{(n)} = e^{-\hat{\lambda}n} F^{(0)} \quad (3.14)$$

As a consequence, the optimal forcing function decreases rapidly with  $n$ , if the largest Lyapunov exponent is much greater than 1. Since  $M = I + \sum_{n=1}^{N-1} M^{(n)}$  we estimate  $\hat{\mu} \approx 1 + \hat{\mu} + \hat{\mu}^2 + \dots + \hat{\mu}^{N-1} = \frac{1-e^{2\hat{\lambda}N}}{1-e^{2\hat{\lambda}}}$ . Then the response can be approximated by

$$R^2 = \frac{1 - e^{2\hat{\lambda}N}}{1 - e^{2\hat{\lambda}}} F^2 \quad (3.15)$$

In comparison, for random forcing  $\mathbf{F}_r^{(n)} = (F_{r,1}^{(n)}, F_{r,2}^{(n)}, \dots, F_{r,d}^{(n)})$  where each component of the forcing function at each time step is a random number with variance  $\langle (F_{r,i}^{(n)})^2 \rangle = F^2/(Nd)$  no correlations  $\langle F_{r,i}^{(n)} F_{r,i}^{(n)} \rangle = 0$  for  $i \neq j$ . Then the expectation value of the response is (from Eq. (3.1), see Eq. (D.3) in the Appendix)

$$R_r^2 = \left( \frac{1}{d} \sum_{i=1}^d \frac{1 - e^{2\lambda_i N}}{1 - e^{2\lambda_i}} \right) \frac{F^2}{N} \quad (3.16)$$

From Eq. (3.15) and Eq. (3.16) we conclude that the response for the optimal forcing is large compared to the response from random forcing if the largest Lyapunov exponent is much larger than the other Lyapunov exponents. Figure 3 shows the response for optimal

forcing and random forcing as a function of the largest Lyapunov exponent for a chaotic shift map dynamics (see Appendix B).

If the unperturbed dynamics is of period  $k$ , i.e.  $\mathbf{y}^{(n+k)} = \mathbf{y}^{(n)}$ , then the Jacobi matrix has the same period, i.e.  $J^{(n+k)} = J^{(n)}$ . Hence  $J^{(n)}J^{(n+1)} \dots J^{(n+k-1)}$  is a constant matrix and the displacement dynamics (Eq. (3.1)) and the dynamics of the resonant forcing function (Eq. (2.7)) have a period- $k$  growth or decay:

$$\mathbf{d}^{(n+k)} = J^{(n+k-1)} J^{(n+k-2)} \dots J^{(n)} \mathbf{d}^{(n)} \quad (3.17)$$

and from Eq. (2.7)

$$\mathbf{F}^{(n+k)} = \left( (J^{(n+k)} J^{(n+k-1)} \dots J^{(n+1)})^T \right)^{-1} \mathbf{F}^{(n)}. \quad (3.18)$$

If  $\{L_i^{(k)}\}$  are the eigenvalues of  $J^{(n+k-1)} J^{(n+k-2)} \dots J^{(n)}$  in Eq. (3.17), then the eigenvalues of  $\left( (J^{(n+k)} J^{(n+k-1)} \dots J^{(n+1)})^T \right)^{-1}$  in Eq. (3.18) are  $\{\tilde{L}_i^{(k)}\} = \{1/L_i^{(k)}\}$ . If we separate the real and imaginary part,  $L_i^k = |L_i^k| e^{i\phi_i^k}$ , and  $\tilde{L}_i^k = |\tilde{L}_i^k| e^{i\tilde{\phi}_i^k}$ , the absolute values  $|L_i^k|$  and  $|\tilde{L}_i^k|$  represent the growth rate and  $\Delta k = |2\pi/\phi_i^k|$  and  $\Delta \tilde{k} = |2\pi/\tilde{\phi}_i^k|$  the period of the dynamics. Since  $\tilde{L}_i^k = \frac{1}{|L_i^k|} e^{-i\phi_i^k}$ , the resonant forcing function  $\mathbf{F}^{(n)}$  and the separation of nearby trajectories  $\epsilon^{(n)}$  have the same period  $\Delta \tilde{k} = \Delta k$ , but inverse growth rates  $\tilde{L}_i^k = 1/L_i^k$ .  $\mathbf{F}^{(0)}$  is not necessarily an eigenvector of  $\left( (J^{(n+k)} J^{(n+k-1)} \dots J^{(n+1)})^T \right)^{-1}$  and some or all periods of the displacement dynamics will show up in the dynamics of the optimal forcing function, but no other periods will be present.

For system with only one variable  $x^{(n+1)} = f(x^{(n)}) + F^{(n)}$ , the eigenvalue of  $M$  is (see Eq. (3.3))

$$\hat{\mu} = 1 + \left( \frac{\partial f}{\partial x} \Big|_{y^{(N-1)}} \right)^2 + \left( \frac{\partial f}{\partial x} \Big|_{y^{(N-1)}} \times \frac{\partial f}{\partial x} \Big|_{y^{(N-2)}} \right)^2 + \dots + \left( \frac{\partial f}{\partial x} \Big|_{y^{(N-1)}} \times \dots \times \frac{\partial f}{\partial x} \Big|_{y^{(1)}} \right)^2 \quad (3.19)$$

From Eq. (3.9) we obtain for the resonant forcing function

$$F^{(n)} = \frac{\partial f}{\partial x} \Big|_{y^{(n+1)}} \times \dots \times \frac{\partial f}{\partial x} \Big|_{y^{(N-2)}} \times \frac{\partial f}{\partial x} \Big|_{y^{(N-1)}} F^{(N-1)} \quad (3.20)$$

where  $F^{(N-1)} = \pm F/\sqrt{\hat{\mu}}$ . The response to the resonant forcing function is  $R = \sqrt{\hat{\mu}}F$ . Figure 4 shows the resonant forcing function (Eq. (3.20)) and the displacement dynamics for a chaotic logistic map dynamics  $x^{(n+1)} = 3.61x^{(n)}(1 - x^{(n)}) + F^{(n)}$ , for  $n = 0, 1, \dots, 14$ , with the initial condition  $y^{(0)} = x^{(0)} = 0.34$ . The magnitude of the forcing function  $F = 0.0001$

is small. With Eq. (3.19) we compute  $\hat{\mu} = 1500$ . We find that the predicted response  $R = 0.00387$  is close to the numerical value  $R = 0.00378$ . Since the map is chaotic, nearby trajectories diverge exponentially on average. The optimal forcing function decreases with the same rate exponentially on average.

#### IV. COMPARISON WITH A SINGLE PUSH FORCING

Next we consider the iterated map dynamics with a single push forcing at the first time step

$$\tilde{\mathbf{x}}^{(n+1)} = \begin{cases} \mathbf{f}(\tilde{\mathbf{x}}^{(n)}) + \tilde{\mathbf{F}}^{(0)} & \text{if } n = 0 \\ \mathbf{f}(\tilde{\mathbf{x}}^{(n)}) & \text{else} \end{cases} \quad (4.1)$$

where  $F^2 = \left(\tilde{\mathbf{F}}^{(0)}\right)^2$ . We use the calculus of variations with Lagrange function  $L$  [17] to determine the forcing function which yields the largest response  $\tilde{R} = (\tilde{\mathbf{x}}^{(N)} - \mathbf{y}^{(N)})^2$ . The Lagrange function is

$$\tilde{L} = \frac{\tilde{R}^2}{2} + \frac{\tilde{\mu}}{2} (\mathbf{F}^{(0)})^2 + \tilde{\mathbf{k}}^{(0)} (\tilde{\mathbf{x}}^{(1)} - \mathbf{f}(\tilde{\mathbf{x}}^{(0)}) - \mathbf{F}^{(0)}) + \sum_{n=1}^{N-1} \tilde{\mathbf{k}}^{(n)} (\tilde{\mathbf{x}}^{(n+1)} - \mathbf{f}(\tilde{\mathbf{x}}^{(n)})) \quad (4.2)$$

where  $\tilde{\mathbf{k}}^{(n)}$ , and  $\tilde{\mu}$  are Lagrange multipliers. The stationary points of the Lagrange function provide a necessary condition for the maximum response. At stationary points the partial derivatives with respect to the components of the independent variables  $\tilde{\mathbf{x}}^{(n)} = (\tilde{x}_1^{(n)}, \tilde{x}_2^{(n)}, \dots, \tilde{x}_d^{(n)})$  and  $\tilde{\mathbf{F}}^{(0)} = (\tilde{F}_1^{(0)}, \tilde{F}_2^{(0)}, \dots, \tilde{F}_d^{(0)})$  are equal to zero.  $\partial L / \partial \tilde{x}_i^{(n)} = 0$  for  $n = 0, 1, \dots, N - 1$  and  $\partial \tilde{L} / \partial \tilde{F}_i^{(0)} = 0$  yield:

$$\begin{aligned} (J^{(n+1)})^T \tilde{\mathbf{k}}^{(n+1)} - \tilde{\mathbf{k}}^{(n)} &= 0 \\ \tilde{\mu} \mathbf{F}^{(0)} - \tilde{\mathbf{k}}^{(0)} &= 0 \end{aligned} \quad (4.3)$$

$\partial \tilde{L} / \partial \tilde{x}_i^{(N)} = 0$  yields:

$$\tilde{\mathbf{x}}^{(N)} - \mathbf{y}^{(N)} + \tilde{\mathbf{k}}^{(N-1)} = 0 \quad (4.4)$$

Next we assume that the forcing function is small and expand the Jacobi matrix about the unperturbed dynamics to lowest order, i.e.  $J^{(n)} \approx (\partial f_i / \partial x_j)|_{\mathbf{y}^{(n)}}$ . To lowest order the difference between the trajectory of the driven system and the unperturbed system reads:

$$\tilde{\mathbf{x}}^{(N)} - \mathbf{y}^{(N)} = J^{(N-1)} \dots J^{(1)} \tilde{\mathbf{F}}^{(0)} \quad (4.5)$$

With Eq. (4.3) we obtain

$$\begin{aligned}\tilde{\mu}\mathbf{x}^{(N)} - \mathbf{y}^{(N)} &= J^{(N-1)} \dots J^{(1)} (J^{(1)})^T \dots (J^{(N-1)})^T \mathbf{k}^{(N-1)} \\ &= \left( J^{(N-1,1)} (J^{(N-1,1)})^T \right) \tilde{\mathbf{k}}^{(N-1)}\end{aligned}$$

With Eq. (4.4) this becomes

$$\tilde{M}\tilde{\mathbf{k}}^{(N-1)} = -\tilde{\mu}\tilde{\mathbf{k}}^{(N-1)} \quad (4.6)$$

where  $\tilde{M} = J^{(N-1,1)} (J^{(N-1,1)})^T$  is a symmetric matrix with up to  $d$  orthogonal eigenvectors  $\tilde{\mathbf{e}}_i$ , where  $\tilde{M}\tilde{\mathbf{e}}_i = \tilde{\mu}_i\tilde{\mathbf{e}}_i$ ,  $i = 1, 2, \dots, d$  and  $\tilde{\mathbf{e}}_i^T \tilde{\mathbf{e}}_i = 1$ . The corresponding eigenvalues  $\tilde{\mu}_i$  are positive. The local Lyapunov exponents are  $\lambda_i = \frac{1}{2(N-1)} \ln \tilde{\mu}_i$ . The eigenvectors of matrix  $\tilde{M}$  are the solutions of Eq. (4.6)  $\tilde{\mathbf{k}}^{(N-1)} = \pm \tilde{k}^{(N-1)} \tilde{\mathbf{e}}_i$ , where  $\tilde{k}^{(N-1)} = |\tilde{\mathbf{k}}^{(N-1)}|$  and  $\tilde{\mu} = -\tilde{\mu}_i$ . In the next few steps we will determine which solutions maximize the response. From Eq. (4.4) we obtain

$$\tilde{R}^2 = (\tilde{\mathbf{x}}^{(N)} - \mathbf{y}^{(N)})^2 = \left( \tilde{k}^{(N-1)} \right)^2 \quad (4.7)$$

Since we know that the final value of the Lagrange multiplier is  $\mathbf{k}^{(N-1)} = \pm k^{(N-1)} \mathbf{e}_i$ , the other values of the Lagrange multiplier are

$$\begin{aligned}\tilde{\mathbf{k}}^{(0)} &= (J^{(1)})^T \tilde{\mathbf{k}}^{(1)} = (J^{(1)})^T (J^{(2)})^T \tilde{\mathbf{k}}^{(2)} = (J^{(1)})^T (J^{(2)})^T \dots (J^{(N-1)})^T \tilde{\mathbf{k}}^{(N-1)} \\ &= (J^{(N-1,1)})^T \tilde{\mathbf{k}}^{(N-1)} = \pm |\tilde{\mathbf{k}}^{(N-1)}| (J^{(N-1,1)})^T \tilde{\mathbf{e}}_i\end{aligned} \quad (4.8)$$

With this equation we determine  $|\tilde{\mathbf{k}}^{(N-1)}|$  as a function of  $F^2$ :

$$\begin{aligned}F^2 &= \left( \tilde{\mathbf{F}}^{(0)} \right)^2 = \left( \tilde{\mathbf{F}}^{(0)} \right)^T \left( \tilde{\mathbf{F}}^{(0)} \right) = \frac{1}{\tilde{\mu}^2} \left( \tilde{\mathbf{k}}^{(0)} \right)^T \left( \tilde{\mathbf{k}}^{(0)} \right) \\ &= \frac{1}{\tilde{\mu}^2} \left( (J^{(N-1,1)})^T \tilde{\mathbf{k}}^{(N-1)} \right)^T \left( (J^{(N-1,1)})^T \tilde{\mathbf{k}}^{(N-1)} \right) = \frac{1}{\tilde{\mu}^2} \left( \tilde{\mathbf{k}}^{(N-1)} \right)^T \tilde{M} \tilde{\mathbf{k}}^{(N-1)} \\ &= \frac{1}{\tilde{\mu}^2} \left( \pm \tilde{k}^{(N-1)} \tilde{\mathbf{e}}_i \right)^T \tilde{M} \left( \pm \tilde{k}^{(N-1)} \tilde{\mathbf{e}}_i \right) = \frac{1}{\tilde{\mu}^2} \left( \tilde{k}^{(N-1)} \right)^2 \tilde{\mathbf{e}}_i^T \tilde{M} \tilde{\mathbf{e}}_i = \frac{1}{\tilde{\mu}^2} \left( \tilde{k}^{(N-1)} \right)^2 \tilde{\mu}_i \\ &= \frac{1}{\tilde{\mu}_i} \left( \tilde{k}^{(N-1)} \right)^2\end{aligned} \quad (4.9)$$

Hence  $\left( \tilde{k}^{(N-1)} \right)^2 = \tilde{\mu}_i F^2$ . With Eq. (4.7) we find  $R^2 = \tilde{\mu}_i F^2$ . Hence for the optimal forcing the final value of the Lagrange parameter  $\tilde{\mathbf{k}}^{(N-1)}$  that is parallel to the eigenvector  $\hat{\mathbf{e}}$  with the largest eigenvalue of  $M$ ,  $\hat{\mu} = \max \{ \tilde{\mu}_i \}$ , produces the largest response. The largest response is

$$\tilde{R} = e^{\hat{\lambda}^{(N-1)} F} \quad (4.10)$$

where  $\hat{\lambda}$  is the largest local Lyapunov exponent. With Eq. (3.4) and Eq. (3.5) we obtain

$$\begin{aligned}\mathbf{F}^{(0)} &= \pm \frac{F}{\exp(\hat{\lambda}(N-1))} (J^{(N-1,1)})^T \hat{\mathbf{e}} \\ &= \pm \frac{F}{\exp(\hat{\lambda}(N-1))} (J^{(1)})^T \dots (J^{(N-2)})^T (J^{(N-1)})^T \hat{\mathbf{e}}\end{aligned}\quad (4.11)$$

where  $\hat{\mathbf{e}}$  is the eigenvector that corresponds to the largest eigenvalue of  $M$ . Figure 5 shows the response for optimal forcing and single push forcing as a function of the largest Lyapunov exponent for a shift map where  $a_2 = 0.5$ ,  $k = 0.2$ ,  $f = 0.001$ , and  $N = 4$ . If the largest Lyapunov exponent is greater than 0.5, the optimal forcing function decreases rapidly with  $n$  (see Eq. (3.14)), and is similar to a single push forcing function.

In comparison, for random single push forcing  $\mathbf{F}_r^{(0)} = (F_{r,1}^{(0)}, F_{r,2}^{(0)}, \dots, F_{r,d}^{(0)})$  each component of the forcing function is a random number with variance  $\langle (F_{r,i}^{(0)})^2 \rangle = F^2/d$ , with no correlations  $\langle F_{r,i}^{(0)} F_{r,j}^{(0)} \rangle = 0$  for  $i \neq j$ . Then the expectation value of the response is (see Eq. (D.4) in the Appendix)

$$R_r^2 = \left( \frac{1}{d} \sum_{i=1}^d e^{2\lambda_i(N-1)} \right) F^2 \quad (4.12)$$

Figure 5 shows the response to a random single push forcing versus the largest Lyapunov exponent.

## V. CONCLUSION

We investigate resonances of chaotic map dynamics. We study the response to forcing functions with a fixed magnitude (see Eq. (2.2) and an arbitrary time dependence. The stationary points of the Lagrange function (Eq. (2.4)) provide necessary conditions (Eq. (2.5), Eq. (2.6)) for an optimal response. From these conditions we derive that the resonant forcing functions complement the separation of nearby trajectories, i.e. the product of the displacement of nearby trajectories and the resonant forcing is a conserved quantity (see Eq. (2.12)). Consequently, when the displacement dynamics is periodic, the resonant forcing function has the same period. Figure 4 shows that the resonant forcing function is irregular if the displacement dynamics is irregular. Eq. (3.14) shows that resonant forcing functions of chaotic systems decrease exponentially, where the rate equals the largest Lyapunov exponent of the unperturbed system. A comparison with the response to random forcing indicates that

the optimal forcing is particularly effective if the largest Lyapunov exponent is significantly larger than the other Lyapunov exponents (see Eq. (3.15) and Eq. (3.16). Figure 5 illustrates that the optimal forcing is only as effective as a single push forcing, if the largest Lyapunov exponent is much larger than unity. In addition to system identification, resonant forcing functions can be used to enhance the response to a periodic forcing functions, like noise may enhance the response to a low frequency periodic forcing function in stochastic resonance[6]. If a system periodically visits the vicinity of the basin of attraction of a multi-attractor system due to a low-frequency periodic forcing, then a small resonant forcing function can push it across the boundary and thus fastly increase the response. The resonant forcing function has the same effect as noise in stochastic resonance, but is resonant forcing are probably much more efficient in ecreasing the response.

In the Appendix we discuss two representative two dimensional systems, the Henon map, and a system with two coupled shift maps.

## VI. APPENDIX

### A. Resonances of the Henon map

For the mapping function

$$\begin{pmatrix} x_1^{(n+1)} \\ x_2^{(n+1)} \end{pmatrix} = \begin{pmatrix} 1 - a(x_1^{(n)})^2 + cx_2^{(n)} + F_1^{(n)} \\ bx_1^{(n)} + F_2^{(n)} \end{pmatrix} \quad (\text{A.1})$$

For  $c = 1$ , the Henon map [18] has two fixed points at  $x_1 = (b - 1 \pm \sqrt{(1 - b)^2 + 4a})/(2a)$  and  $x_2 = bx_1$  for  $a > a_0 = -(1 - b)^2/4$ . One fixed point is always unstable and the other is unstable if  $a < a_1 = 3(1 - b)^2/4$ . For  $a_0 < a < a_1$  the trajectories are attracted to the stable fixed point. For  $a > a_1$  the map has a period-k attractor where k increases with a and becomes infinite at  $a_\infty$ .  $a_\infty$  depends on  $b$ . For  $b = 0.3$ , Henon found  $a_\infty \approx 1.06$ . For  $a_\infty < a < 1.55$  the dynamics is chaotic with periodic windows. In addition the map has more than one attractor with fractal basins of attraction for certain a-values. For example for  $a = 1.07$  and  $b = 0.3$  the two initial states  $(x_1^{(0)}, x_2^{(0)}) = (1, 0)$  and  $(1.5, 0)$  go to different limiting sets. The first initial condition goes to a strange attractor, whereas the second initial condition goes to a period-6 attractor. For  $b = c = 0$ , the Henon map becomes the

logistic map. The Jacobian matrix is

$$J^{(n)} = \begin{pmatrix} -2ax_1^{(n)} & c \\ b & 0 \end{pmatrix} \quad (\text{A.2})$$

For  $N = 2$  the matrix  $M$  is

$$M = \begin{pmatrix} 1 + c^2 + 4a^2(x_1^{(1)})^2 & -2abx_1^{(1)} \\ -2abx_1^{(1)} & 1 + b^2 \end{pmatrix} \quad (\text{A.3})$$

where  $x_1^{(1)} = 1 - a(x_1^{(0)})^2 + x_2^{(0)}$ . The largest eigenvalue of  $M$  is

$$\hat{\mu} = \frac{1}{2} \left( 2 + b^2 + c^2 + 4a^2(x_1^{(1)})^2 + \sqrt{b^4 - 2b^2(c^2 - 4a^2(x_1^{(1)})^2) + (c^2 + 4a^2(x_1^{(1)})^2)^2} \right) \quad (\text{A.4})$$

and the corresponding eigenvector of  $M$  is

$$\hat{\mathbf{e}} = (s, -4abx_1^{(1)}) / \sqrt{s^2 + (4abx_1^{(1)})^2} \quad (\text{A.5})$$

where

$$s = c^2 - b^2 + 4a^2(x_1^{(1)})^2 + \sqrt{b^4 - 2b^2(c^2 - 4a^2(x_1^{(1)})^2) + (c^2 + 4a^2(x_1^{(1)})^2)^2} \quad (\text{A.6})$$

With Eq. (3.6) we find

$$\mathbf{F}^{(1)} = \pm \frac{F}{\sqrt{\hat{\mu}}} \hat{\mathbf{e}} = \pm \frac{F}{\sqrt{\hat{\mu} (s^2 + (4abx_1^{(1)})^2)}} (s, -4abx_1^{(1)}) \quad (\text{A.7})$$

and

$$\mathbf{F}^{(0)} = \pm \frac{F}{\sqrt{\hat{\mu} (s^2 + (4abx_1^{(1)})^2)}} (-2ax_1^{(1)}(s + 2b^2), sc) \quad (\text{A.8})$$

With Eq. (3.7) we find

$$R^2 = \frac{F^2}{2} \left( 2 + b^2 + c^2 + 4a^2(x_1^{(1)})^2 + \sqrt{b^4 - 2b^2(c^2 - 4a^2(x_1^{(1)})^2) + (c^2 + 4a^2(x_1^{(1)})^2)^2} \right) \quad (\text{A.9})$$

The expectation value of the response is

$$\begin{aligned}
R^2 &= \left\langle \frac{F^2}{2} \left( 2 + b^2 + c^2 + 4a^2 \left( x_1^{(1)} \right)^2 + \right. \right. \\
&\quad \left. \left. \sqrt{b^4 - 2b^2 \left( c^2 - 4a^2 \left( x_1^{(1)} \right)^2 \right) + \left( c^2 + 4a^2 \left( x_1^{(1)} \right)^2 \right)^2} \right) \right\rangle \\
&\approx \frac{F^2}{2} \left( 2 + b^2 + c^2 + 4a^2 \left\langle \left( x_1^{(1)} \right)^2 \right\rangle + \right. \\
&\quad \left. \sqrt{b^4 - 2b^2 \left( c^2 - 4a^2 \left\langle \left( x_1^{(1)} \right)^2 \right\rangle \right) + \left( c^2 + 4a^2 \left\langle \left( x_1^{(1)} \right)^2 \right\rangle \right)^2} \right) \tag{A.10}
\end{aligned}$$

where  $\langle \left( x_1^{(1)} \right)^2 \rangle$  is averaged over the attractor.

For the logistic map [18], i.e. if  $b = c = 0$  then  $\hat{\mu} = 1 + 4a^2 \left( x_1^{(1)} \right)^2$ ,  $\hat{\mathbf{e}} = (1, 0)$ ,  $\mathbf{F}^{(1)} = \pm (F/\sqrt{\hat{\mu}}, 0)$ ,  $\mathbf{F}^{(0)} = \pm (-ax_1^{(1)}F/\sqrt{\hat{\mu}}, 0)$ , and

$$R = F \sqrt{1 + 4a^2 \left( x_1^{(1)} \right)^2} \tag{A.11}$$

where  $x^{(1)}$  is a function of the initial condition  $x_1^{(0)}$ , i.e.  $x_1^{(1)} = 1 - a \left( x_1^{(0)} \right)^2$ . These results are in agreement with Eq. (3.19) and Eq. (3.20).

## B. Resonances of coupled shift maps

For the mapping function

$$\begin{pmatrix} x_1^{(n+1)} \\ x_2^{(n+1)} \end{pmatrix} = \begin{pmatrix} \text{mod}(a_1 x_1^{(n)} + k x_2^{(n)} + F_1^{(n)}) \\ \text{mod}(a_2 x_2^{(n)} + k x_1^{(n)} + F_2^{(n)}) \end{pmatrix} \tag{B.1}$$

The Jacobian matrix is

$$J^{(n)} = \begin{pmatrix} a_1 & k \\ k & a_2 \end{pmatrix} \tag{B.2}$$

where the function  $\text{mod}(x)$  returns the decimal part of  $x$ .  $a_1$  and  $a_2$  are the growth rates and  $k$  is the coupling constant. We assume that  $a_1 > a_2 \geq 0$ . The eigenvalues of  $M^{(1)}$  are  $\mu_{1/2}^{(1)} = 0.5(a_1^2 + a_2^2 + 2k^2 \pm (a_1 + a_2)\sqrt{(a_1 - a_2)^2 + 4k^2})$  and the eigenvectors  $\mathbf{e} = (a_1 - a_2 \pm \sqrt{(a_1 - a_2)^2 + 4k^2}, 2k) / \sqrt{((a_1 - a_2 \pm \sqrt{(a_1 - a_2)^2 + 4k^2})^2 + 4k^2)}$ . If  $\hat{\mu} > 1$  the unperturbed dynamics is chaotic. Since  $J^{(n)}$  is symmetric and constant, the eigenvectors

of the  $M^{(1)}$  are eigenvectors of  $M^{(n)}$ , and the Lyapunov exponents are  $\lambda_{1/2} = \frac{1}{2} \ln \mu_{1/2}^{(1)}$  and the largest Lyapunov exponent is  $\hat{\lambda} = \lambda_1$ . Hence

$$\begin{aligned}
& M\hat{\mathbf{e}} \\
&= (I + \sum_{n=1}^{N-1} J^{(N-1,n)} (J^{(N-1,n)})^T) \hat{\mathbf{e}} \\
&= (I + \sum_{n=1}^{N-1} (J^{(N-1,n)})^2) \hat{\mathbf{e}} \\
&= (I + \sum_{n=1}^{N-1} (J)^{2N-2n}) \hat{\mathbf{e}} \tag{B.3} \\
&= (I + \sum_{n=1}^{N-1} (J)^{2n}) \hat{\mathbf{e}} \\
&= (1 + \sum_{n=1}^{N-1} e^{2n\hat{\lambda}}) \hat{\mathbf{e}} \\
&= (\sum_{n=0}^{N-1} e^{2n\hat{\lambda}}) \hat{\mathbf{e}} \\
&= \frac{e^{2N\hat{\lambda}} - 1}{e^{2\hat{\lambda}} - 1} \hat{\mathbf{e}}
\end{aligned}$$

With Eq. (3.5) we find

$$\mathbf{F}^{(n)} = (J^{(n+1)})^T \dots (J^{(N-2)})^T (J^{(N-1)})^T \hat{\mathbf{F}}^{N-1} = \pm (J)^{N-1-n} \frac{F}{\sqrt{\hat{\mu}}} \hat{\mathbf{e}} \tag{B.4}$$

With Eq. (3.14) we find

$$R^2 = F^2 \frac{e^{2N\hat{\lambda}} - 1}{e^{2\hat{\lambda}} - 1} \tag{B.5}$$

If  $k = 0$  then  $\hat{\mu}_J = a_1$ ,  $\hat{\mu} = \frac{a_1^{2N-1}}{a_1^2-1}$ ,  $\hat{\mathbf{e}} = (1, 0)$ ,  $\mathbf{F}^{(n)} = \pm (a_1^{N-n-1} F / \sqrt{\hat{\mu}}, 0) = (F^{(0)} / a_1^n, 0)$ , where  $F^{(0)} = \pm a_1^{N-1} F / \sqrt{\hat{\mu}}$  and

$$R = F \sqrt{\frac{a_1^{2N} - 1}{a_1^2 - 1}} \tag{B.6}$$

For  $k = 0$  the system contains two decoupled shift maps, where  $\lambda_i = \ln |a_i|$ ,  $i = 1, 2$  is the Lyapunov exponent of each map. The resonant forcing function is in the direction of the map with the larger Lyapunov exponent. Hence if both maps have a positive Lyapunov exponent and therefore both are chaotic, then the resonant forcing function forces only the map which is more chaotic. There is no forcing of the less chaotic map.

### C. Several Proofs

Proof of Eq. (3.2):

$$\begin{aligned}
\mathbf{x}^{(N)} - \mathbf{y}^{(N)} &= \mathbf{F}^{(N-1)} + J^{(N-1)} (J^{(N-1)})^T \mathbf{F}^{(N-1)} + \\
&J^{(N-1)} J^{(N-2)} (J^{(N-2)})^T (J^{(N-1)})^T \mathbf{F}^{(N-1)} + \dots + \\
&J^{(N-1)} \dots J^{(1)} (J^{(1)})^T \dots (J^{(N-1)})^T \mathbf{F}^{(N-1)} \\
&= \mathbf{F}^{(N-1)} + M^{(1)} \mathbf{F}^{(N-1)} + \\
&M^{(2)} \mathbf{F}^{(N-1)} + \dots + M^{(N-1)} \mathbf{F}^{(N-1)} \\
&= \left( I + \sum_{n=1}^{N-1} M^{(n)} \right) \mathbf{F}^{(N-1)} \\
&= M \mathbf{F}^{(N-1)}
\end{aligned} \tag{D.1}$$

Proof of Eq. (3.6):

$$\begin{aligned}
F^2 &= (\mathbf{F}^{(N-1)})^2 + (\mathbf{F}^{(N-2)})^2 + \dots + (\mathbf{F}^{(0)})^2 \\
&= (\mathbf{F}^{(N-1)})^T (\mathbf{F}^{(N-1)}) + (\mathbf{F}^{(N-2)})^T (\mathbf{F}^{(N-2)}) + \dots + (\mathbf{F}^{(0)})^T (\mathbf{F}^{(0)}) \\
&= (\mathbf{F}^{(N-1)})^T (\mathbf{F}^{(N-1)}) + \sum_{n=0}^{N-2} (\mathbf{F}^{(n)})^T (\mathbf{F}^{(n)}) \\
&= (\mathbf{F}^{(N-1)})^T (\mathbf{F}^{(N-1)}) + \sum_{n=0}^{N-2} \left( (J^{(n+1)})^T (J^{(n+2)})^T \dots (J^{(N-1)})^T \mathbf{F}^{(N-1)} \right)^T \cdot \\
&\quad \left( (J^{(n+1)})^T (J^{(n+2)})^T \dots (J^{(N-1)})^T \mathbf{F}^{(N-1)} \right) \\
&= (\mathbf{F}^{(N-1)})^T (\mathbf{F}^{(N-1)}) + \\
&+ \sum_{n=0}^{N-2} (\mathbf{F}^{(N-1)})^T J^{(N-1)} \dots J^{(n+2)} J^{(n+1)} (J^{(n+1)})^T (J^{(n+2)})^T \dots (J^{(N-1)})^T \mathbf{F}^{(N-1)} \\
&= (\mathbf{F}^{(N-1)})^T \left( I + \sum_{n=1}^{N-1} M^{(n)} \right) \mathbf{F}^{(N-1)} \\
&= (\mathbf{F}^{(N-1)})^T M \mathbf{F}^{(N-1)} \\
&= (\pm F^{(N-1)} \mathbf{e}_i)^T M (\pm F^{(N-1)} \mathbf{e}_i) \\
&= (F^{(N-1)})^2 \mathbf{e}_i^T M \mathbf{e}_i \\
&= (F^{(N-1)})^2 \mu_i \\
&= \mu_i (F^{(N-1)})^2
\end{aligned} \tag{D.2}$$

Proof of Eq. (3.16):

$$\begin{aligned}
R_r^2 &= \langle (\mathbf{F}_r^{(N-1)} + J^{(N-1)}\mathbf{F}_r^{(N-2)} + \\
&+ J^{(N-1)}J^{(N-2)}\mathbf{F}_r^{(N-3)} + \dots + J^{(N-1)}J^{(N-2)}\dots J^{(1)}\mathbf{F}_r^{(0)})^2 \rangle = \\
&= \langle (\mathbf{F}_r^{(N-1)})^T \mathbf{F}_r^{(N-1)} \rangle + \langle (\mathbf{F}_r^{(N-2)})^T M^{(1)} \mathbf{F}_r^{(N-2)} \rangle + \\
&+ \langle (\mathbf{F}_r^{(N-3)})^T M^{(2)} \mathbf{F}_r^{(N-3)} \rangle + \dots + \langle (\mathbf{F}_r^{(0)})^T M^{(N-1)} \mathbf{F}_r^{(0)} \rangle = \\
&= \langle (\mathbf{F}_r^{(N-1)})^T \mathbf{F}_r^{(N-1)} \rangle + \langle \sum_{i=1}^d ((\mathbf{F}_r^{(N-2)} \mathbf{e}_i) \mathbf{e}_i)^T M^{(1)} \sum_{i=1}^d (\mathbf{F}_r^{(N-2)} \mathbf{e}_i) \mathbf{e}_i \rangle + \\
&+ \langle \sum_{i=1}^d ((\mathbf{F}_r^{(N-3)} \mathbf{e}_i) \mathbf{e}_i)^T M^{(2)} \sum_{i=1}^d (\mathbf{F}_r^{(N-3)} \mathbf{e}_i) \mathbf{e}_i \rangle + \dots + \\
&+ \langle \sum_{i=1}^d ((\mathbf{F}_r^{(0)} \mathbf{e}_i) \mathbf{e}_i)^T M^{(N-1)} \sum_{i=1}^d (\mathbf{F}_r^{(0)} \mathbf{e}_i) \mathbf{e}_i \rangle = \\
&= \langle \sum_{i=1}^d (\mathbf{F}_{r,i}^{(N-1)})^2 \rangle + \langle \sum_{i=1}^d ((\mathbf{F}_r^{(N-2)} \mathbf{e}_i) \mathbf{e}_i)^T \sum_{i=1}^d \mu_i^{(1)} (\mathbf{F}_r^{(N-2)} \mathbf{e}_i) \mathbf{e}_i \rangle + \\
&+ \langle \sum_{i=1}^d ((\mathbf{F}_r^{(N-3)} \mathbf{e}_i) \mathbf{e}_i)^T \sum_{i=1}^d \mu_i^{(2)} (\mathbf{F}_r^{(N-3)} \mathbf{e}_i) \mathbf{e}_i \rangle + \dots + \\
&+ \langle \sum_{i=1}^d ((\mathbf{F}_r^{(0)} \mathbf{e}_i) \mathbf{e}_i)^T \sum_{i=1}^d \mu_i^{(N-1)} (\mathbf{F}_r^{(0)} \mathbf{e}_i) \mathbf{e}_i \rangle = \tag{D.3} \\
&= \sum_{i=1}^d \frac{F^2}{dN} + \langle \sum_{i=1}^d ((\mathbf{F}_r^{(N-2)} \mathbf{e}_i) \mu_i^{(1)} (\mathbf{F}_r^{(N-2)} \mathbf{e}_i) \rangle + \\
&+ \langle \sum_{i=1}^d (\mathbf{F}_r^{(N-3)} \mathbf{e}_i) \mu_i^{(2)} (\mathbf{F}_r^{(N-3)} \mathbf{e}_i) \rangle + \dots + \\
&+ \langle \sum_{i=1}^d (\mathbf{F}_r^{(0)} \mathbf{e}_i) \mu_i^{(N-1)} (\mathbf{F}_r^{(0)} \mathbf{e}_i) \rangle = \\
&= \frac{F^2}{N} + \langle \sum_{i=1}^d \mu_i^{(1)} (\mathbf{F}_r^{(N-2)} \mathbf{e}_i)^2 \rangle + \\
&+ \langle \sum_{i=1}^d \mu_i^{(2)} (\mathbf{F}_r^{(N-3)} \mathbf{e}_i)^2 \rangle + \dots + \langle \sum_{i=1}^d \mu_i^{(N-1)} (\mathbf{F}_r^{(0)} \mathbf{e}_i)^2 \rangle =
\end{aligned}$$

$$\begin{aligned}
&= \frac{F^2}{N} + \sum_{i=1}^d \mu_i^{(1)} \langle (\mathbf{F}_r^{(N-2)} \mathbf{e}_i)^2 \rangle + \\
&\quad + \sum_{i=1}^d \mu_i^{(2)} \langle (\mathbf{F}_r^{(N-3)} \mathbf{e}_i)^2 \rangle + \cdots + \\
&\quad\quad + \sum_{i=1}^d \mu_i^{(N-1)} \langle (\mathbf{F}_r^{(0)} \mathbf{e}_i)^2 \rangle = \\
&= \frac{F^2}{N} + \sum_{i=1}^d \mu_i^{(1)} \langle \sum_{j=1}^d (F_{r,j}^{(N-2)})^2 (e_{i,j})^2 \rangle + \sum_{i=1}^d \mu_i^{(2)} \langle \sum_{j=1}^d (F_{r,j}^{(N-3)})^2 (e_{i,j})^2 \rangle + \cdots + \\
&\quad\quad\quad + \sum_{i=1}^d \mu_i^{(N-1)} \langle \sum_{j=1}^d (F_{r,j}^{(0)})^2 (e_{i,j})^2 \rangle = \\
&= \frac{F^2}{N} + \sum_{i=1}^d \mu_i^{(1)} \sum_{j=1}^d \langle (F_{r,j}^{(N-2)})^2 \rangle (e_{i,j})^2 + \sum_{i=1}^d \mu_i^{(2)} \sum_{j=1}^d \langle (F_{r,j}^{(N-3)})^2 \rangle (e_{i,j})^2 + \cdots + \\
&\quad\quad\quad + \sum_{i=1}^d \mu_i^{(N-1)} \sum_{j=1}^d \langle (F_{r,j}^{(0)})^2 \rangle (e_{i,j})^2 = \\
&= \frac{F^2}{N} + \sum_{i=1}^d \mu_i^{(1)} \frac{F^2}{Nd} + \sum_{i=1}^d \mu_i^{(2)} \frac{F^2}{Nd} + \cdots + \sum_{i=1}^d \mu_i^{(N-1)} \frac{F^2}{Nd} = \\
&= \frac{F^2}{Nd} \sum_{i=1}^d (1 + \mu_i^{(1)} + \mu_i^{(2)} + \cdots + \mu_i^{(N-1)}) = \\
&= \frac{F^2}{Nd} \sum_{i=1}^d (1 + \mu_i + \mu_i^2 + \cdots + \mu_i^{N-1}) = \\
&= \frac{F^2}{Nd} \sum_{i=1}^d \frac{1 - \mu_i^N}{1 - \mu_i}
\end{aligned}$$

where  $e_{i,j}$  is the  $j$ -th component of the  $i$ -th eigenvector of  $M^{(1)}$ .

Proof of Eq. (4.12)

$$R_r^2 = \langle (J^{(N-1)} J^{(N-2)} \dots J^{(1)} \mathbf{F}_r^{(0)})^2 \rangle =$$

$$\begin{aligned}
& = \langle (\mathbf{F}_r^{(0)})^T M^{(N-1)} \mathbf{F}_r^{(0)} \rangle = \\
& = \langle \sum_{i=1}^d ((\mathbf{F}_r^{(0)} \mathbf{e}_i) \mathbf{e}_i)^T M^{(N-1)} \sum_{i=1}^d (\mathbf{F}_r^{(0)} \mathbf{e}_i) \mathbf{e}_i \rangle = \\
& = \langle \sum_{i=1}^d ((\mathbf{F}_r^{(0)} \mathbf{e}_i) \mathbf{e}_i)^T \sum_{i=1}^d \mu_i^{(N-1)} (\mathbf{F}_r^{(0)} \mathbf{e}_i) \mathbf{e}_i \rangle = \\
& = \langle \sum_{i=1}^d ((\mathbf{F}_r^{(0)} \mathbf{e}_i) \mu_i^{(N-1)} (\mathbf{F}_r^{(0)} \mathbf{e}_i)) \rangle = \\
& = \langle \sum_{i=1}^d \mu_i^{(N-1)} (\mathbf{F}_r^{(0)} \mathbf{e}_i)^2 \rangle = \\
& = \sum_{i=1}^d \mu_i^{(N-1)} \langle (\mathbf{F}_r^{(0)} \mathbf{e}_i)^2 \rangle = \\
& = \sum_{i=1}^d \mu_i^{(N-1)} \langle \sum_{j=1}^d (F_{r,j}^{(0)})^2 (e_{i,j})^2 \rangle = \\
& = \sum_{i=1}^d \mu_i^{(N-1)} \sum_{j=1}^d \langle (F_{r,j}^{(0)})^2 \rangle (e_{i,j})^2 = \\
& = \sum_{i=1}^d \mu_i^{(N-1)} \frac{F^2}{d} = \\
& = \frac{F^2}{d} \sum_{i=1}^d \mu_i^{(N-1)} = \\
& = \frac{F^2}{d} \sum_{i=1}^d \mu_i^{N-1}
\end{aligned}$$

## Acknowledgments

This material is based upon work supported by the National Science Foundation Grant No. NSF PHY 01-40179 and NSF DMS 03-25939 ITR. A.H. thanks the Santa Fe Institute for support.

---

- [1] A. H. Nayfeh and D. T. Mook, *Nonlinear Oscillations* (Wiley, New York, 1979).
- [2] J. Guckenheimer and P. Holmes, *Nonlinear Oscillations, Dynamical Systems, and Bifurcations of Vector Fields* (Springer, New York, 1983).
- [3] A. J. Lichtenberg and M. A. Lieberman, *Regular and Stochastic Motion* (Springer, New York, 1991).
- [4] T. Eisenhammer, A. Hubler, T. Geisel, and E. Luscher, *Phys. Rev. A* **41**, 3332 (1990).
- [5] I. Siddiqi, R. Vijay, F. Pierre, C. M. Wilson, L. Frunzio, M. Metcalfe, C. Rigettiand, R. J. Schoelkopf, M. H. Devoret, D. Vion, et al., *Phys. Rev. Lett.* **94**, 027005 (2005).
- [6] R. L. Badzey and P. Mohanty, *Nature* **437**, 962 (2005).
- [7] S. Wimberger, R. Mannella, O. Morsch, and E. Arimondo, *Phys Rev Lett.* **94**, 130404 (2005).
- [8] D. Ruelle, *Phys. Rev. Lett.* **56**, 405 (1986).
- [9] E. Ott, C. Grebogi, and J. A. Yorke, *Phys. Rev. Lett.* **64**, 1196 (1990).
- [10] N. Baba, A. Amann, E. Scholl, and W. Just, *Phys. Rev. Lett.* **89**, 074101 (2002).
- [11] S. M. Soskin, R. Mannella, and P. V. E. McClintock, *Phys. Rep.* **373**, 247 (2003).
- [12] S. M. Soskin, O. M. Yevtushenko, and R. Mannella, *Phys. Rev. Lett.* **95**, 224101 (2005).
- [13] B. B. Plapp and A. W. Hubler, *Phys. Rev. Lett.* **65**, 2302 (1990).
- [14] S. Krempf, T. Eisenhammer, A. Hubler, G. Mayer-Kress, and P. W. Milonni, *Phys. Rev. Lett.* **69**, 430 (1992).
- [15] C. Wargitsch and A. Hubler, *Phys. Rev. E* **51**, 1508 (1995).
- [16] K. Chang, A. Kodogeorgiou, A. W. Hubler, and E. A. Jackson, *Physica D* **51**, 99 (1991).
- [17] I. N. Bronshtein and K. A. Semendyayev, *Handbook of Mathematics* (H. Deutsch, Thun, 1985).
- [18] E. Ott, *Chaos in Dynamical Systems* (Cambridge University Press, Cambridge, 1993).

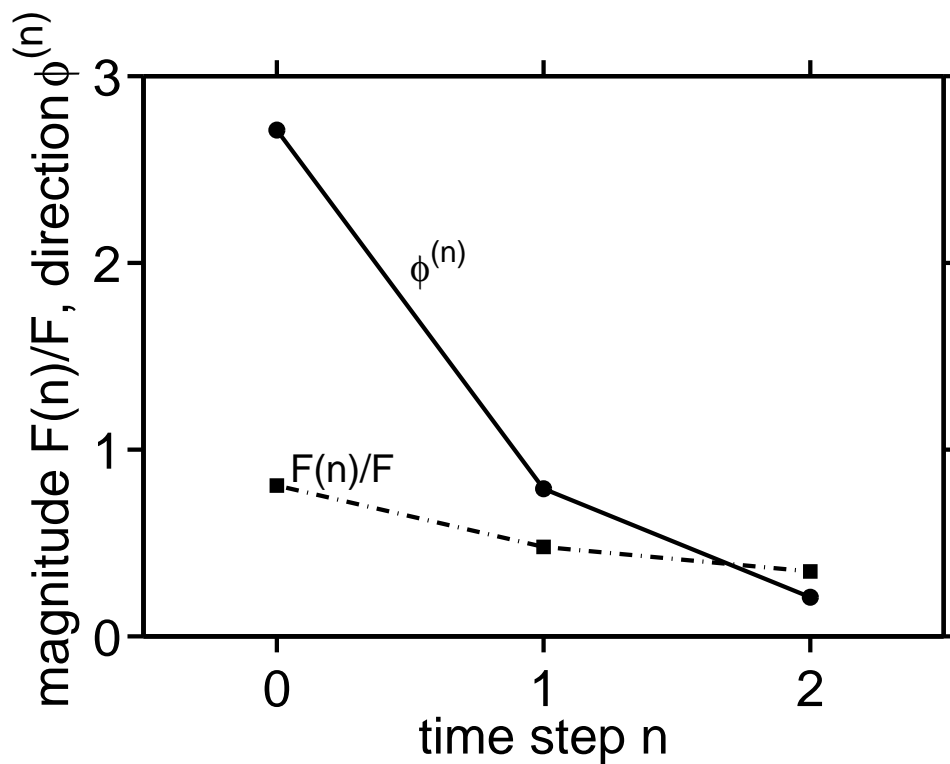


FIG. 1: The relative magnitude of resonant forcing  $F^{(n)}/F$  (squares) and the direction  $\phi^{(n)}$  of the resonant forcing function (circles) versus time for a chaotic Henon map dynamics. The scalar product of the resonant forcing function and the displacement is a conserved quantity, i.e.  $\mathbf{F}^{(n)} \cdot \mathbf{d}^{(n)} = \text{constant}$ .

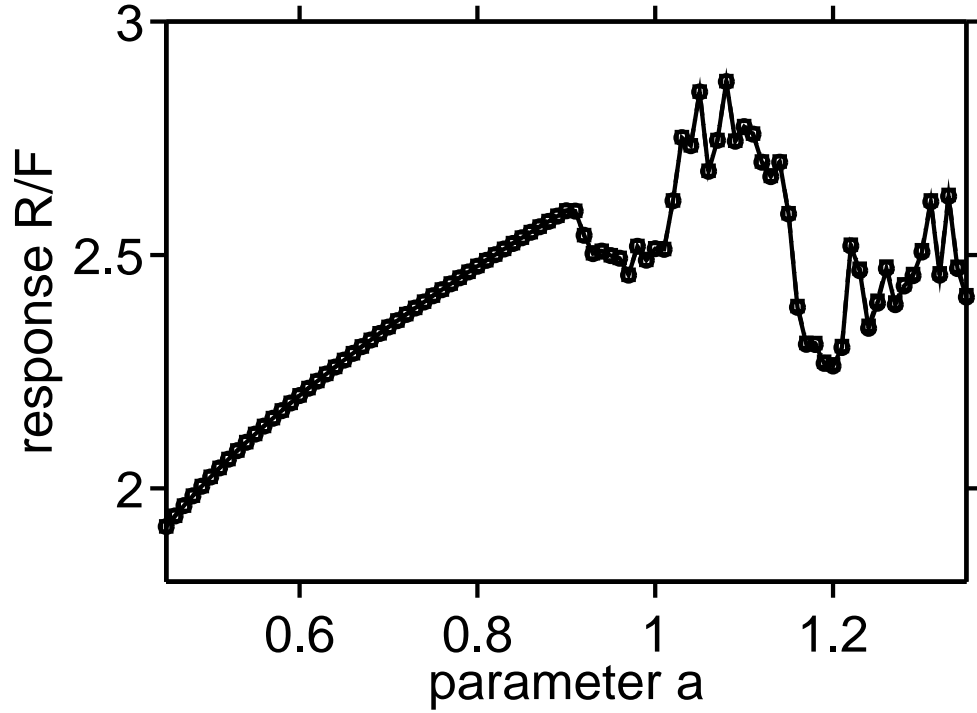


FIG. 2: The expectation value of the response to a resonant forcing function versus the parameter  $a$  of a Henon map, where  $N = 2$ ,  $b = 0.3$ ,  $c = 1$ , and  $F = 0.001$ . The squares indicate numerical results. The continuous line is the theoretical value given by Eq. (A.10), where the expectation value  $\langle (x_1^{(1)})^2 \rangle$  is computed numerically.

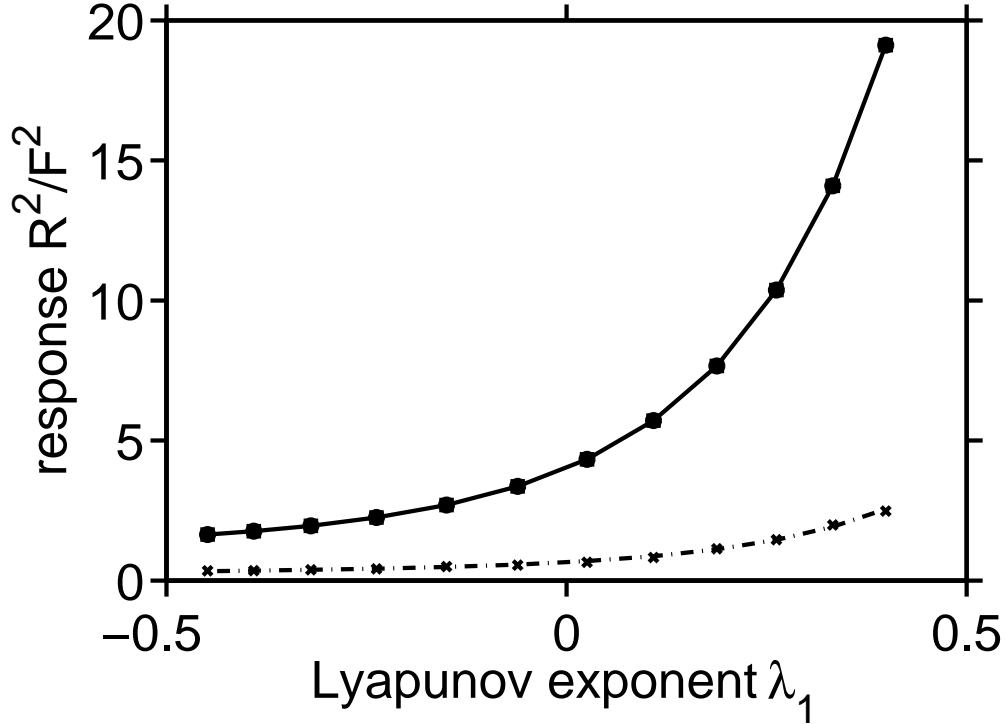


FIG. 3: The response  $R^2/F^2$  to a resonant forcing function versus the largest Lyapunov exponent  $\lambda_1 = \hat{\lambda}$  of a shift map, where  $N = 4$ ,  $a_2 = 0.5$ ,  $k = .2$ , and  $F = 0.0001$ . The squares indicate numerical results. The continuous line is the theoretical value given by Eq. (3.15). The dashed line is the expectation value response to a random forcing function (Eq. (3.16)) and the x-labels indicate numerical results. This figure illustrates that the optimal forcing function is particularly efficient if one Lyapunov exponent is significantly larger than the others.

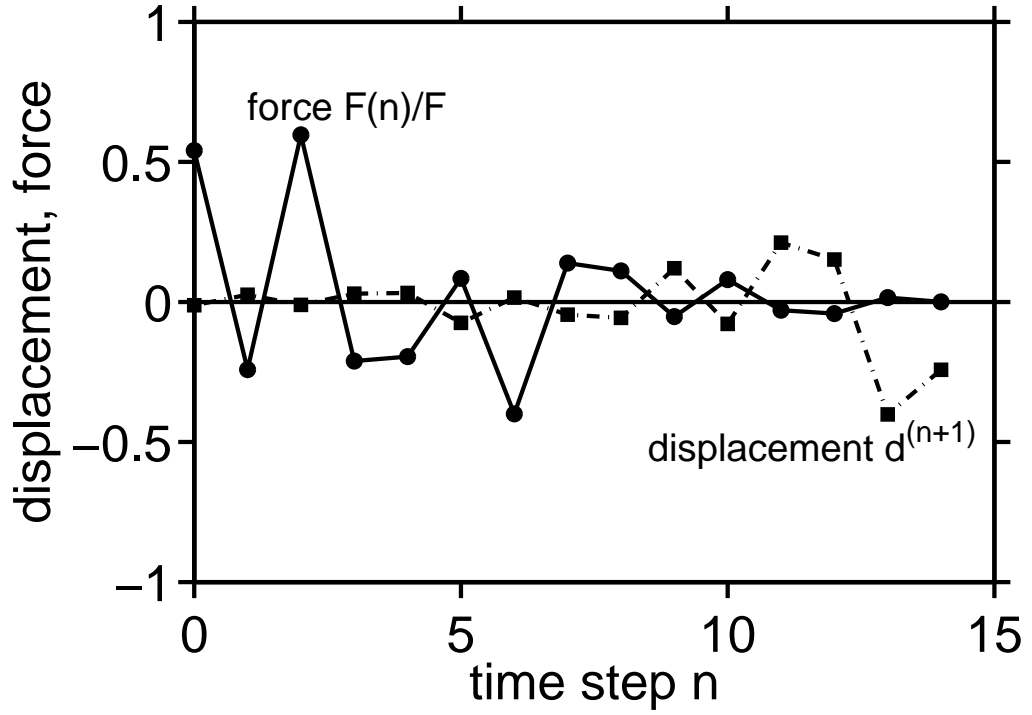


FIG. 4: The resonant forcing  $F^{(n)}$  (circles) and the displacement of two neighboring trajectories  $d^{(n+1)}$  (squares) versus time step  $n$  for a chaotic logistic map dynamics. This plot illustrates that the resonant forcing complements the displacement of neighboring trajectories of the unperturbed system, i.e.  $F^{(n)}d^{(n+1)} = \text{constant}$ . When the magnitude of the displacement is large, then the magnitude of the resonant force is small, and if the displacement is positive, the resonant force is negative.

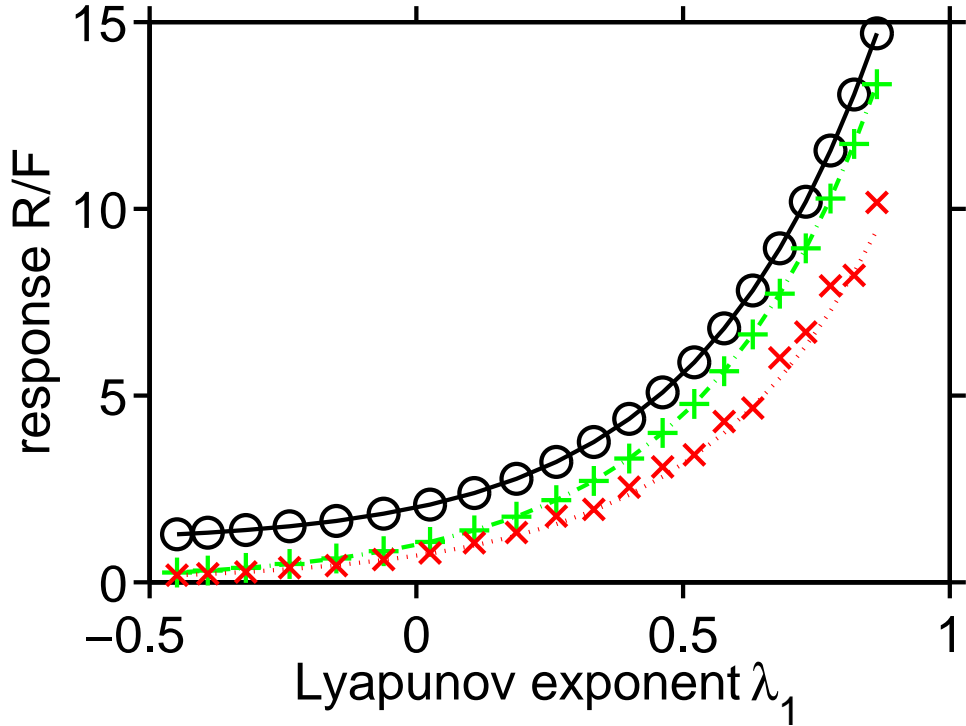


FIG. 5: The response  $R/F$  of a shift map to an optimal forcing function versus the largest Lyapunov exponent  $\hat{\lambda} = \lambda_1$ , where the continuous line is the theoretical value (Eq. (3.15)) and the bullets are numerical values. The dashed line is the response to an optimal single push forcing (Eq. (4.10)) and the plus markers are numerical values. For small Lyapunov exponents the responses to the optimal forcing is by a factor of five larger, whereas for large Lyapunov exponents the difference in the response decreases to a few percent since the optimal forcing function becomes similar to a single push forcing function. The dotted line is the response to a random single push forcing (Eq. (4.12)) and the cross markers are numerical estimates of the expectation value of the response.